24nd IMEKO TC4 International Symposium
Electrical & Electronic Measurements Promote Industry 4.0
September 17-20, 2019，Xi'an, China

Electrical Characteristics of Pantograph Arcs in DC Railways: Infrastructure Influence

A. Mariscotti[1], D. Giordano[2]

[1]*ASTM Sagl, Chiasso, Switzerland, andrea.mariscotti@astm-e.ch*
[2]*Istituto Nazionale di Ricerca Metrologica (INRIM), Torino, Italy, d.giordano@inrim.it*

***Abstract* – Electric arcs are an unavoidable by-product of current collection by sliding contact in electrified transportation systems. Electric arcs are transient phenomena with implications for PQ measurements and wearing estimation and prevention of the sliding contact and catenary. Besides being heavily influenced by mechanical characteristics and material properties, their electrical characterization encompasses spectral properties and the influence of train and traction line circuits and relative position of infrastructure elements. This paper identifies the influence of such electrical and system characteristics onto the spectral signature of electric arcs for DC railways.**

***Keywords* – Arc discharge, Electric arc, Power Quality, Rail transportation**

I. INTRODUCTION

The objective of this work is the characterization of the electric behavior of the electric arc at the pantograph-catenary interface of DC railway vehicles, using electrical quantities, namely the pantograph voltage and current. Important parameters are the duration of the arc transient, its rate of rise and the peak voltage variation. A secondary objective is the characterization in terms of the speed and absorbed current. The importance of electric arc characterization is manifold: the number of electric arcs is recalled as an index of current collection quality in the EN 50367 [1] (percentage of arcing, sec. 7.3); a significant arc activity implies rapid wearing of the pantograph sliding contact [2][3], as well as a far from ideal catenary system; the arc itself is a source of electromagnetic emissions over a broad frequency range [4], possibly disturbing radio devices e.g. used for signaling or telecommunication [5][6]; last, electric arc transients disturb the measurement of other electrical quantities for assessment of power quality and power absorption [7]-[9].

II. ELECTRIC ARC CHARACTERISTICS

A typical V-I characteristic of a DC arc can be summarized as follows: at very low current (tens of amperes) a behavior defined by a constant arc power law can be observed; for currents higher than a specific threshold, the voltage level reaches a plateau and does not depend any longer on the current value. Various V-I arc characteristic curves for DC low-voltage arcs with static electrodes were provided by Paukert's [10]: he collected data provided by seven research institutes for current ranging from 100 A to 100 kA [7].

The dynamic behavior of the electric arc depends on some relevant factors: the train speed, wind speed and its direction, the intensity of the flowing current for which a slight adaptation of the voltage-resistance model is always necessary [11]-[14]. However results available in the literature almost always refer to AC systems.

III. CATENARY – PANTOGRAPH ELECTRIC INTERACTION

Simpler models using a single pi cell for the representation of the traction line and fixing the inductance and capacitance values to a predetermined line section length were proposed in [12]-[14]. Having observed repeated resonance oscillations supposedly triggered by electric arc events, this paper proposes a more complex model: the electric behavior of a traction line at the pantograph-contact line interface may be predicted by the simpler equations shown in [15] or by more elaborated expressions, based on a mixed representation of traction line and loading networks [16].

The line response is characterized by a first resonance that does not depend on the train position between two substations, taken as electric terminations of the traction line section, under the assumption that, thanks to the substation output capacitors, the short circuit impedance of the substation at the dc output terminals is much less than that of the adjacent line sections. Anti-resonances of the line impedance Z_p at the pantograph have variable frequency changing with the position of the moving train (see (1)).

$$Z_p = Z_c \frac{\tanh(\gamma x L)\tanh[\gamma(1-x)L]}{\tanh(\gamma x L)+\tanh[\gamma(1-x)L]} \qquad (1)$$

where Z_c is the line characteristic impedance [15], x is the train position and L the overall length of the line section between the two terminating substations (see Fig. 2).

When excited by the electric arc, the transient response of the line should manifest in principle in all the electrical quantities of the circuit as a set of oscillation modes related to resonance or anti-resonance frequencies. Depending on the associated resistive value, damping will be more or less significant. The phenomenon is analyzed by means of a distributed parameters model of the traction line including substation Z_{ESS} [17]. The train is modeled by means of its input filter (no equivalent resistance for the traction and auxiliaries absorbed power as its effect is masked by the filter capacitor already at very low frequency). The electric arc is modeled as the series connections of a generator and a resistor, simulating the arc resistance.

The model is implemented in a compact Matlab code used for line response study [16][17] using transmission line equations for the traction line (implementing a distributed parameter model including line losses, due to e.g. skin effect in the running rails) and lumped Kirchhoff equations circuits for the terminal conditions (substations and train). The electric and line parameters considered as the basic configuration for the successive sensitivity analyses are shown in Table 1.

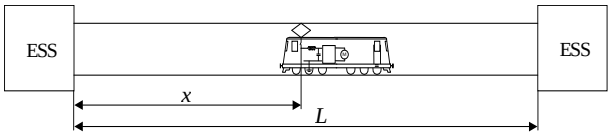

Fig. 1. Block description of the circuit model

Table 1. Onboard filter parameters of some rolling stock

Rolling stock	L_f	C_f	$f_{self\,res}$
E402B	16 mH	3.2 mF	22.2 Hz
E412	21 mH	9.47 mF	11.3 Hz
TAF	18 mH	2.5 mF	23.7 Hz
ETR460	21 mH	4 mF	17.4 Hz

A. Influence of the train position

Train position measured between two substations (ESS), that are known to represent terminal conditions for signals at about 100 Hz or higher, influences directly the anti-resonance frequencies at high frequency, but not the location of the resonance peak of the Z_p impedance. In general, due to the high frequency of the first line anti-resonance, and the relatively large equivalent line resistance, there is not such a big excursion of values between the line resonance and anti-resonance along the Z_p curve.

Three sets of curves are shown in Fig. 2 for three different lengths of the line section between two ESSs, with four curves corresponding to four different train positions x measured relative to ESS-ESS separation L: x=0.1, 0.2, 0.33, 0.5L. Positions beyond mid point at 0.5L and symmetric to those of the interval 0-0.5L give identical results.

The resonance peak is always positioned at a frequency independent on train position, but on line section length L [16]. Conversely, the height of the resonance peak Z_r is influenced by the train position.

$$\omega_r(k,L)=\frac{k\pi\upsilon_0}{L} \tag{1}$$

$$Z_r=Z(\omega_r)=\frac{Z_c}{2}\frac{1-\cos(2k\pi x/L)}{\alpha L} \tag{2}$$

where α is the line attenuation constant [16].

The anti-resonance frequency depends on train position. The Z_p value at anti-resonance theoretically depends on train position, but by a combination of factors it is only slightly affected, as shown in Fig. 2.

$$\omega_a(k,x,L)=\frac{k\pi\upsilon_0}{x},\ \frac{k\pi\upsilon_0}{(L-x)}\quad Z_a=Z(\omega_a)=\begin{cases}Z_c\alpha x\\ Z_c\alpha(L-x)\end{cases} \tag{3}$$

The factor of merit at resonance is quite large, in the range of 12 to 15, so with a significant effect in terms of pantograph voltage amplification when excited by electric arc transient.

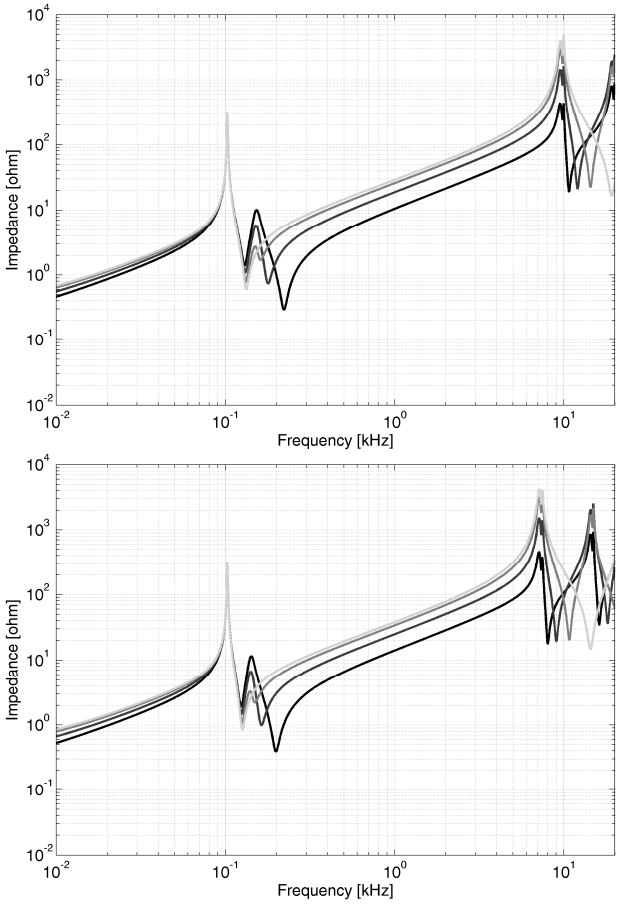

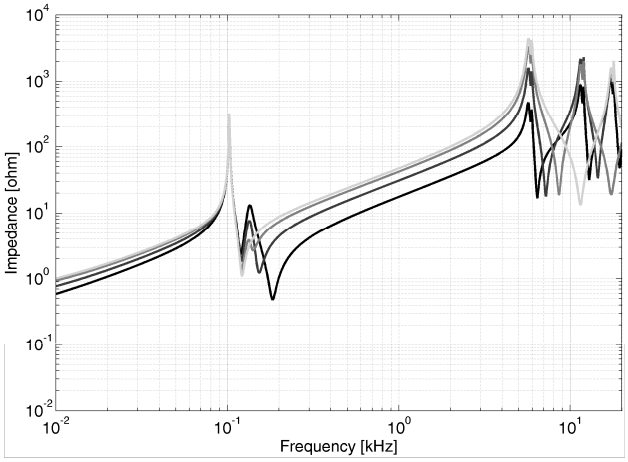

Fig. 2. Z_p for three ESSs separations L: (top) 15 km, (mid) 20 km, (bot) 25 km; no vehicle filter; four train positions (from black to light grey) x=0.1, 0.2, 0.33, 0.5 L

The low frequency resonance/anti-resonance is caused by the ESS filter and may be slightly variable depending on the implemented values of inductance and capacitance. As a consequence, a significant 100 Hz component is visible, generated by the ESS rectifier.

At high frequency the distribution of the anti-resonance frequency is variable and evenly distributed approximately between 6.5 and 20 kHz, depending on the separation of the substations and the train position between them. On average, considering also the double anti-resonance for the longest line L=25 km, we may say that the anti-resonance is located halfway, that is between 12 and 15 kHz. The pantograph current will show a persistent response at this frequency continuously excited by various types of transients and high frequency components, including the steep front of the electric arc event.

The different damping values are remarked, where between the 120 Hz substation-induced anti-resonance and the high-frequency anti-resonances there is a difference of about 20 of resistive values.

B. Onboard equivalent circuit and input filter effect

The input filter on-board vehicles is a low-pass LC filter with typical resonance between 10 and 20 Hz. Whatever the loading (as equivalent resistance in parallel to the capacitor), the shunting effect is negligible for frequencies above some tens of Hz; for this reason only the LC on-board filter is considered. The on-board filter is in parallel with Z_p when seen from the pantograph port. Ideally speaking, its loading effect is negligible for frequencies above a hundred Hz, since the filter inductance is larger than the total line inductance for lengths up to about 25-30 km. As shown in Fig. 3 a wide variability of curve is visible up to 100 Hz; from here onward there is only a negligible shift between curves.

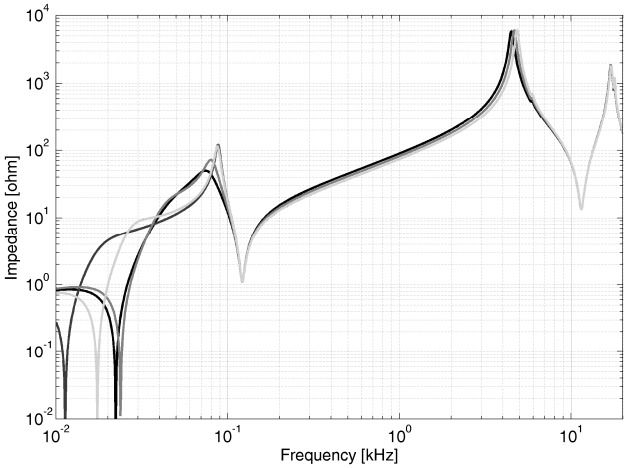

Fig. 3. Sensitivity analysis of Z_p for varying vehicle input filter: E402B, E412, TAF, ETR460 (see Table 1).

C. Influence of the variable electric arc resistance

The electric arc is a dynamic phenomenon with a variable arc resistance during the occurrence of the transient. Electric arc resistance values have been estimated for dc arcs at various inter-electrode gaps. Arc resistance R_a is in general negligible as shown in [3], Fig. 14, where values of 10 to 100 mΩ are reported. In case of various types of wearing after long use, surface electric contact worsens with maximum ten times higher values [18]. Observed values during preliminary measurements [7] are of the same order (about 0.2 to 0.5 Ω).

The arc resistance is always in series with Z_p, for what regards the equivalent circuit of pantograph voltage and current, occurring at the sliding contact interface, whereas the two electrical quantities are measured on the roof and inside the rolling stock. However, even larger arc resistance values will not cause any appreciable change of the overall series impedance and flowing current, being small compared to the overall line resistance and reactance (see the Z_p values in Fig. 2).

IV. EXPERIMENTAL RESULTS

Contrarily to the band-pass recordings presented in [5][6], with large sample rate and focus on electric field emissions, the measurements used here were done in base-band, using voltage and current probes connected to the pantograph: 50 kS/s sample rate and probe bandwidth of about 20 kHz, suitable to follow the arc ignition, its rate of change and successive oscillations (see Fig. 4).

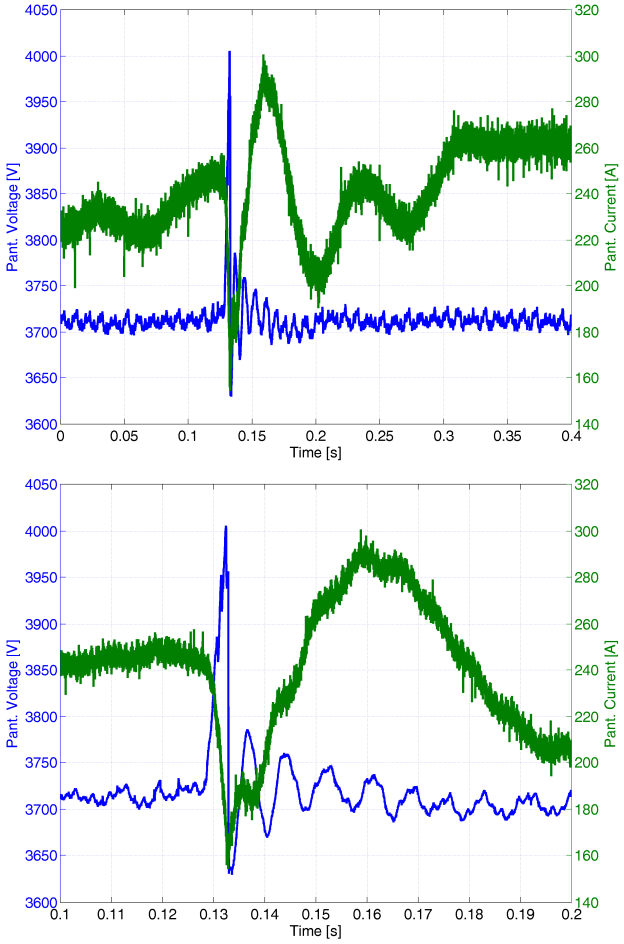

Fig. 4. Electric arc event during braking: pantograph voltage and current recordings of a 3 kV DC line.

As shown in Fig. 4, the arc event triggers voltage oscillations at a frequency slightly larger than 100 Hz (around 0.14-0.15 s), corresponding to the predicted anti-resonance of Fig. 2; such faster oscillations (at about 120 Hz) are damped and disappear in about five cycles, and the regular 100 Hz resumes (e.g. beyond 0.19 s). The first peak of the current is caused by the excitation of the on-board filter and ESS anti-resonances, visible in Fig. 2 and 3 at about 10-30 and 120-150 Hz. The broader oscillation that follows the current peak is due to the transient response of the on-board filter tuned to about 15 Hz, not visible in the voltage waveform besides a slight fluctuation due to the very low voltage line impedance and, as a consequence, voltage drop.

The persistent low-frequency oscillations on the pantograph voltage (caused by the substation ripple mainly at 100 and 300 Hz) hide the high-frequency components that should be located at line resonances, that are visible only with a more detailed spectral analysis. To narrow the analysis across the arc event, considering the short duration of the arc, the larger damping at high frequency, and the underlying low-frequency components that cause local non-stationarity of the extracted time windows, tools with a short time support and yet sufficient frequency resolution are needed: suitable tools may be wavelets and joint time-frequency transforms.

V. CONCLUSIONS

This paper has presented the problem of pantograph electric arc characterization in DC railway systems using site recordings of pantograph quantities (voltage V_p and current I_p). For a general approach the influence of the infrastructure and vehicle filter shall be considered, determining the degree of variability affecting the mentioned quantities, or a derived representation, i.e. the pantograph impedance $Z_p=V_p/I_p$. The impact of such variability has been evaluated for the quantities of interest.

The experimental verification has shown that the electric arc interact with the pantograph line impedance, causing voltage oscillations in agreement with the modelled Z_p curves. The smaller oscillations of the I_p current are also in agreement with the proposed model.

The purpose of the characterization of electric arcs can be synthesized as done in the Introduction: identification of such events as a measure of current collection quality and in general to predict the degree of wearing of materials and contact surfaces; quantification of Power Quality degradation in relation to electric arc events and to the triggered phenomena, such as system oscillations. The observed phenomena at the catenary-pantograph interface are indeed present in the return circuit in terms of return current; so, the analysis of the evolution of the spectral components associated to electric arc events can pinpoint possible issues of interference to signaling devices through the track.

VI. ACKNOWLEDGMENT

The results here presented are developed in the framework of the 16ENG04 MyRailS Project, funded by the European Union's Horizon 2020 research and innovation program. This work was supported by the Swiss State Secretariat for Education, Research and Innovation (SERI) under contract number 17.00127. The opinions expressed and arguments employed herein do not necessarily reflect the official views of the Swiss Government.

REFERENCES

[1] CENELEC EN 50367, *Railway applications – Current collection systems – Technical criteria for the interaction between pantograph and overhead line (to achieve free access)*, 2016.

[2] Guangning Wu, Wenfu Wei, Guoqiang Gao, Jie Wu and Yue Zhou, "Evolution of the electrical contact of dynamic pantograph–catenary system," *Journal of Modern Transportation*, 2016, vol. 24, n. 2, pp. 132-138.

[3] G. Bucca, A. Collina, "A procedure for the wear prediction of collector strip and contact wire in pantograph–catenary system," *Wear*, vol. 266, 2009, pp. 46-59.

[4] G. Gao, X. Yan, Z. Yang, W. Wei, Y. Hu, and G. Wu, "Pantograph–Catenary Arcing Detection Based on

Electromagnetic Radiation," *IEEE Trans. on Electromagnetic Compatibility*, vol. 99, 2018, pp. 1-7.

[5] S. Dudoyer, V. Deniau, S. Ambellouis, M. Heddebaut and A. Mariscotti, "Classification of Transient EM Noise Depending on their Effect on the Quality of GSM-R Reception," *IEEE Trans. on Electromagnetic Compatibility*, vol. 55, n. 5, Oct. 2013, pp. 867-874.

[6] A. Mariscotti, A. Marrese, N. Pasquino and R. Schiano-Lo Moriello, "Time and frequency characterization of radiated disturbance in telecommunication bands due to pantograph arcing," *Measurement*, vol. 46, 2013, pp. 4342-4352.

[7] G. Crotti et al., "Pantograph-to-OHL Arc: Conducted Effects in DC Railway Supply System," *IEEE Trans. on Instrumentation and Measurement*, (in print) 2019.

[8] A. Mariscotti, "Characterization of Power Quality transient phenomena of DC railway traction supply", *ACTA IMEKO*, July 2012, vol. 1, n. 1, pp. 26-35.

[9] R. F. Ammerman and P. K. Sen, "Modeling High-Current Electrical Arcs: A Volt-Ampere Characteristic Perspective for AC and DC Systems," 2007 39th North American Power Symposium, Las Cruces, NM, 2007, pp. 58-62.

[10] Paukert, J. "The Arc Voltage and the Resistance of LV Fault Arcs," 7th International conference, Switching arc phenomena; 1993; Lodz; Poland, pp 49-51.

[11] G. Gao, T. Zhang, W. Wei, Y. Hu, G. Wu and N. Zhou, "A pantograph arcing model for electrified railways with different speeds," *Proc IMechE, Part F: Journal of Rail and Rapid Transit*, vol. 232, n. 6, 2017, pp. 1731-1740.

[12] J. L. Guardado, S. G. Maximov, E. Melgoza, J. L. Naredo and P. Moreno, "An Improved Arc Model Before Current Zero Based on the Combined Mayr and Cassie Arc Models," *IEEE Trans. on Power Delivery*, vol. 20, n. 1, Jan. 2005, pp. 138-142.

[13] Zhou Hongyi, Liu Zhigang, Cheng Ye and Huang Ke, "Extended black-box model of pantograph arcing considering varying pantograph detachment distance," IEEE Transportation Electrification Conference and Expo (ITEC Asia-Pacific), Aug. 7-10, 2017, Harbin, China.

[14] F. M. Uriarte, A. L. Gattozzi, J. D. Herbst, H. B. Estes, T.J. Hotz, A. Kwasinski and R. E. Hebner, "A DC Arc Model for Series Faults in Low Voltage Microgrids," *IEEE Trans. on Smart Grid*, vol. 3, n. 4, Dec. 2012, pp. 2063-2070.

[15] J. Holtz and H. J. Klein, "The propagation of harmonic currents generated by inverter fed locomotives in the distributed overhead supply systems," *IEEE Trans. Power Electronics*, vol. 4, pp. 168–174, Apr. 1989.

[16] A. Mariscotti, P. Pozzobon, "Synthesis of line impedance expressions for railway traction systems", *IEEE Trans. on Vehicular Technology*, vol. 52 n. 2, March 2003, pp. 420-430.

[17] P. Ferrari, A. Mariscotti, P. Pozzobon "Reference curves of the pantograph impedance in DC railway systems", IEEE International Conference on Circuits and Systems, Geneve, Switzerland, May 28-31, 2000, pp. I-555/558.

[18] V. V. Terzija and H. J. Koglin, "On the Modeling of Long Arc in Still Air and Arc Resistance Calculation", *IEEE Trans. on Power Delivery*, Vol. 19, n. 3, July 2004, pp. 1012-1017.